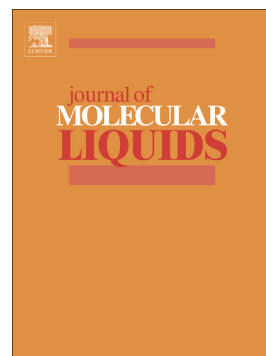


Journal Pre-proof

Virtual spectral histopathology of colon cancer - biomedical applications of Raman spectroscopy and imaging

Beata Brozek-Pluska, Adam Dziki, Halina Abramczyk



PII: S0167-7322(19)35461-3

DOI: <https://doi.org/10.1016/j.molliq.2020.112676>

Reference: MOLLIQ 112676

To appear in: *Journal of Molecular Liquids*

Received date: 1 October 2019

Revised date: 6 February 2020

Accepted date: 10 February 2020

Please cite this article as: B. Brozek-Pluska, A. Dziki and H. Abramczyk, Virtual spectral histopathology of colon cancer - biomedical applications of Raman spectroscopy and imaging, *Journal of Molecular Liquids*(2020), <https://doi.org/10.1016/j.molliq.2020.112676>

This is a PDF file of an article that has undergone enhancements after acceptance, such as the addition of a cover page and metadata, and formatting for readability, but it is not yet the definitive version of record. This version will undergo additional copyediting, typesetting and review before it is published in its final form, but we are providing this version to give early visibility of the article. Please note that, during the production process, errors may be discovered which could affect the content, and all legal disclaimers that apply to the journal pertain.

© 2020 Published by Elsevier.

Virtual spectral histopathology of colon cancer - biomedical applications of Raman spectroscopy and imaging

Beata Brozek-Pluska ^{a,*}, Adam Dziki ^b, Halina Abramczyk ^a

^a Laboratory of Laser Molecular Spectroscopy, Institute of Applied Radiation Chemistry, Lodz University of Technology, Wroblewskiego 15, 93-590 Lodz, Poland.

^b Department of General and Colorectal Surgery, Medical University of Lodz, University Clinical Hospital the Military Medical Academy - Central Veterans' Hospital, Haller Square 1, 90-647 Lodz, Poland

* Corresponding author at: Laboratory of Laser Molecular Spectroscopy, Institute of Applied Radiation Chemistry, Lodz University of Technology, Wroblewskiego 15, 93-590 Lodz, Poland. E-mail address: beata.brozek-pluska@p.lodz.pl

Abstract

Colon cancer is one of the most commonly detected pathology and is the third worldwide cause of death in the US and Europe and ranks second with regard to the incidence of malignant tumors in population. Raman spectroscopy and imaging can be used for colon cancer detection and bioanalytical characterization of noncancerous and pathologically changed tissues. These studies included Raman spectroscopy measurement of not fixed and not stained tissues samples. Presented study included patients from Poland, who were ≥ 18 years of age and underwent colon cancer surgery. Outcomes were measured using confocal Raman microscope, spectroscopy results were compared with traditional histopathology analysis outcomes. DNA, lipids, proteins and carotenoids can be treated as biomarkers of cancerogenesis. Ratios: 751/1156 (DNA/Carotenoids), 1228/1332 (β -sheet/ α -helix proteins conformation), 1586/1004 (Phosphorylated proteins/Proteins), 2854/2935 (Lipids/Proteins) can be used to differentiate noncancerous and cancerous human sigmoid colon mucosa based on Raman spectroscopy and imaging. We have proved that Raman spectroscopy and imaging are a powerful technique to distinguish between noncancerous and cancerous human sigmoid colon mucosa and to characterize biochemical composition of multilayer sigmoid colon tissues samples.

Keywords: Colon cancer, Raman spectroscopy, Raman imaging, cancer biomarkers, diagnostics

1. Introduction

Nowadays Raman spectroscopy and imaging have been recognized as a powerful tool in bioanalytical, biochemical and medical applications. High sensitivity and specificity, above 90%, especially related to the fingerprint region of Raman spectra, offer precise identification of biomarkers based on their unique vibrations. The great advantage of Raman spectroscopy and imaging is also related to the fact that samples analysis doesn't require any staining, which is beneficial in terms of time-consuming protocols and analysis costs.

As a consequence, Raman based methods including Raman spectroscopy and imaging have emerged in last years as one of the most important alternatives for traditional *ex vivo* human tissue examination by H&E staining and highly efficient tool for biomedical applications [1-11]. A considerable progress in the field of *in vivo* - clinical assessment, especially due to the spectroscopic fiber technologies is also observed [12, 13].

Colon cancer, one of the most commonly detected pathology is the third worldwide cause of death with mortality around 60% in the United States and Europe and ranks second with regard to the incidence of malignant tumors in population [14].

The main endoscopic examination used in clinical practice for colon cancer screening is colonoscopy. However, colonoscopy has some disadvantages and risk such as colonic perforation occurring in approximately 1 in 1000 cases, or hemorrhagic complications that may occur during or after colonoscopy. When combined with anesthesia, other difficulties may include cardiovascular complications such as a temporary drop in blood pressure, the risk of blood clots, pulmonary embolism or deep vein thrombosis. In rare cases, more serious cardio-pulmonary disorders may occur including heart attack, stroke and even death. From a biochemical point of view the colonoscopy does not provide answer about origin of tissue abnormality. The suspicious lesion as they may be potentially cancerous, must be removed and further analyzed by trained pathologist by using the gold standard staining protocols that are particularly time consuming, subjective, and high skills personnel demanding. All mentioned above reasons stimulate researchers around the world to develop new tools that enable *ex vivo* as well as *in vivo* diagnostics to fit into the clinical practice less time-consuming protocols to predict the cancer pathology of imaged human biopsies automatically by computing real-time virtual histology images based not only on morphological but as well as biochemical features [4-7].

In this paper we will focus on Raman based diagnostic of large intestine, sigmoid part (*Latin sigmoideum*). In generally large intestine is the end section of the colon of the

vertebrates connecting the small intestine with the anus. In this part of the digestive tract the final stage of absorption of water, electrolytes and mineral salts from the food occurs. The name of this large intestine segment comes from its shape, reminiscent of the letter "S". Sigmoid colon is initially directed with a convex arch to the right side and then turns down going into the rectum and has a long meandering and turns. Scheme 1 presents the cross section of the sigmoid colon. One can see from the Scheme 1 that sigmoid colon includes: a colonic crypts, a mucous membrane, which does not form intestinal villi, but which is also strongly undulated (it effectively increases its surface area) and which consists of one or more layers of epithelial cells overlying a layer of loose connective tissue, a submucosa, a muscle layers and a serosa.

Sch. 1 The cross-section through the layers of the sigmoid human colon.

Typically, the content of human large intestine is a diverse mix of bile, mucus, various microorganisms, feed fermentation products, unabsorbed food and its metabolic products including toxins, mutagens, and dissolved gases. That's a reason why the colon mucosa is constantly exposed to different oxidants, what may then lead to uncontrolled oxidative stress, DNA damage, and finally cancer development.

The first *in-vivo* Raman measurements of human gastrointestinal tissue were published in 2000 by Shim et al. [15]. This study has shown that fiber-optic-coupled Raman spectroscopy can be successfully used for disease classification during *in-vivo* measurements. FT-Raman studies of colorectal cancers have been published also by Andrande et al. [16]. Authors described a diagnostic algorithm useful to establish the spectral differences of the complex colon tissues to find characteristic Raman features. The first Raman and CARS data of colon tissue were published by Krafft et al. [17]. Authors showed CARS images, whose were recorded from thin colon tissue sections at 2850, 1660, 1450 and 1000 cm^{-1} and compared with Raman images obtained using classical spontaneous scattering Raman effect. Comparison between CARS and spontaneous Raman images confirmed that results obtained using both methods are comparable, but a time needed for CARS maps acquisition is three orders of magnitude shorter. In 2013 Gerwert et al. [18] have shown that the auto-fluorescence of colon tissue overlaps spatially with the fluorescence of antibodies against p53, which are of interest in routine immunohistochemistry in pathology analysis and indicates nuclei with mutated p53 of cancer cells. They have also shown many advantages of VIS region (532 nm) excitation compared to excitations wavelengths from IR region (785 or 830 nm) most often used in spectroscopic experiments [18].

In this manuscript we will focus on biochemical composition of healthy and cancerous changed human sigmoid mucosa. We will show that Raman spectroscopy and imaging can be used for bioanalytical characterization of noncancerous and pathologically changed tissues and that analysis of lipids, proteins profiles and other components content of noncancerous and cancerous tissues of a human sigmoid colon based on their Raman spectra can help to understand metabolic pathways in human body and can be useful in determination of spectroscopic biomarkers for clinical practice.

2. Experimental

2.1. Sample preparation

Tissue samples were collected during the routine surgery. The non-fixed, fresh samples were used to prepare 16 micrometers sections. Specimens of the tissue from the tumor mass and the tissue from the safety margin outside of the tumor mass were prepared for Raman analysis by placing specimens on CaF₂ windows. Adjacent sections were used for typical histological analysis.

All tissue procedures were conducted under a protocol approved by the institutional Bioethical Committee at the Medical University of Lodz, Poland (RNN/323/17/KE/17/10/2017). Written informed consent was obtained from patients. Details of the sample preparation and the research methodology have been described in detail in our previous papers [5-7]. The number of patients in our database is equal to 30.

2.2. Raman spectroscopy and imaging

All Raman images and spectra reported in this manuscript were recorded using alpha 300 RSA+ confocal microscope (WITec, Ulm, Germany) using a 50 μm core diameter fiber, an Ultra High Throughput Spectrometer and a CCD Camera Andor Newton DU970NUVB- 353 operating in standard mode with 1600×200 pixels at -60 °C with full vertical binning. 532 nm excitation line - the second harmonic of the Nd:YAG laser was focused on the sample through a 40x dry objective (Nikon, objective type CFI Plan Fluor C ELWD DIC-M, numerical aperture (NA) of 0.60 and a 3.6–2.8 mm working distance). The average laser excitation power was 10 mW. During Raman measurements the grating with 1200 grooves/mm was centered in two positions: at 900 cm^{-1} to record the low frequency region and 2900 cm^{-1} to record the high frequency region, for each measurement the integration time was 0.5 sec. An edge filter was used to remove the Rayleigh scattered light. A piezoelectric table was used to record Raman images. Spectra were collected at one acquisition per pixel

and 1200 lines per mm diffraction grating. The cosmic rays were removed from each Raman spectrum (model: filter size: 2, dynamic factor: 10) and the smoothing procedure: Savitzky–Golay method (model: order: 4, derivative: 0) was also implemented. Data acquisition and processing were performed using WITec Project Plus [5-7]. All imaging data were analyzed using Cluster Analysis (CA) method. Briefly CA allows to group a set of objects (vibrational spectra in our studies) in such a way that to the same group called a cluster belong objects that are more similar to each other (in a sense of vibrational features in our case) than to those in other groups (another clusters). CA was performed using WITec Project Plus, model: Centroid - the k-means algorithm (each cluster was represented by a single mean vector). Data were normalized using Origin software (normalization model: divided by norm).

3. Results and discussion

In this section we will present the results for human sigmoidal colon cancer and human sigmoidal noncancerous tissues from the same patient. Before we formulate general conclusions that may be useful in medical diagnostic, we will provide a data for the patient marked with a symbol PB in our database, to discuss the most important research observations regarding the chemical composition of noncancerous and cancerous sigmoid mucosa. We will present typical average Raman spectra based on thousands of spectra recorded in our measurements.

Figure 1 presents the HE and microscopy image (A), Raman image constructed by CA method (B) and Raman spectra typical for all clusters (C) for noncancerous (I) and cancerous (II) human mucosa of sigmoid colon.

Fig.1 (I) *The microscopy image (A), Raman image (150x150 μm , spatial resolution 2 μm , integration time 0.5 sec.) constructed based on Cluster Analysis method (B) and Raman spectra typical for all clusters (C) for noncancerous human mucosa of sigmoid colon; (II) The microscopy image (A), Raman image (150x150 μm , spatial resolution 2 μm , integration time 0.5 sec.) constructed based on Cluster Analysis method (B) and Raman spectra typical for all clusters (C) for cancerous human mucosa of sigmoid colon, patient PB.*

One can see from Fig. 1 panels IA and IB that Raman images reproduce perfectly the morphology of analyzed tissue, and colors of clusters can be easy associated with different substructures of sample, for example adipose cells are illustrated in panel IB in blue, while

epithelial tissue is shown in red. Red and orange colors in panel IIB show epithelial tissue of cancerous sample.

In Fig. 1 one can see also that Raman peaks typical for epithelial and adipose cells of human sigmoid mucosa can be observed at: 751, 873, 959, 1004, 1156, 1270, 1376, 1448, 1521, 1586, 1653, 2657, 2854, 2900, 2928, 3012 cm^{-1} for the noncancerous tissue, panel IC and at: 751, 1004, 1127, 1171, 1228, 1342, 1365, 1396, 1448, 1557, 1586, 1635, 2875, 2905, 2935, 2964 cm^{-1} for the cancerous one, panel IIC. All observed peaks are characteristic for: DNA/RNA, lipids, saturated and unsaturated fatty acids and their derivatives (esters), phospholipids, and proteins. Table 1 presents the tentative assignments of Raman peaks observed for both types of samples including those which differentiate the noncancerous and the cancerous tissues of human sigmoid colon mucosa [4-7, 10, 11].

Wavenumber [cm^{-1}]	Tentative assignments	Type of human sigmoid colon tissue
751	Nucleic acids, Trp	N, C
873	Amino acids, polysaccharides, collagen	N
959	Hydroxyproline/Collagen backbone	N
1004	Phenylalanine, sym. ring breathing of protein	N, C
1127	Saturated fatty acid	C
1156	beta-carotene C-C stretching mode	N
1171	Tyrosine (collagen type I)	C
1228	Proteins b-sheet conformation	C
1270	Amide III, α -helix	N
1342	DNA/RNA	C
1365	Tryptophan	C
1376	DNA/RNA bases	N
1396	CH rocking	C
1448	Lipids/Proteins	C
1521	beta-carotene C-C stretching mode	N
1557	Amide II, proteins, amide II β -sheet	C
1586	Phosphorylated amino acids and proteins	N, C
1635	Collagen	C
1653	Unsaturated fatty acids, triglycerides, Amide I α helix	N
2854	Fatty acids, triglycerides, C-H ₂ sym. str.	N
2875	Lipids and proteins	C
2900-2905	Lipids and proteins	N, C
2928	Proteins	N
2935	Proteins and lipids, chain end CH ₃ symmetric band	C
2964	C-H vibrations of the acetyl groups	C
3012	=C-H, lipids, unsaturated fatty acids	N

Table 1 The tentative assignments of Raman peaks observed for both types of sigmoid mucosa samples and those which differentiate the noncancerous and the cancerous tissues of sigmoid colon human mucosa [4-7, 10, 11], N-noncancerous tissue, C-cancerous tissue of sigmoid colon human mucosa.

In generally the Raman spectra are very sensitive to variable biochemical environment especially in low frequency region called “fingerprint region” that’s why Raman imaging can easily illustrate the inhomogeneous distribution of various chemical components in tissues samples. Due to the inhomogeneity of distribution of chemical components of tissues the Raman spectra vary greatly depending on the imaging area chosen for the analysis. To minimize this effect, we computed the average Raman spectra for each cluster within the analyzed area of recorded images.

Figure 2 presents the average Raman spectra based on 5600 single Raman spectra typical for noncancerous and cancerous human sigmoid mucosa and the difference spectrum (to show reliable differences between the noncancerous and the cancerous Raman spectra we removed fluorescence from the spectra of human sigmoid mucosa cancer).

Fig. 2. The average Raman spectra typical for noncancerous (blue line) and cancerous (red line) human sigmoid colon mucosa based on 5600 single Raman spectra and the difference spectrum; model: noncancerous-cancerous.

Figure 2 shows that the main differences between the spectra of noncancerous and cancerous sigmoid human mucosa can be found for: nucleic acids DNA/RNA (peaks at 751, 1342 cm^{-1}), fatty acids-saturated fraction (peak at 1127 cm^{-1}), collagen type I (peak at 1171 cm^{-1}), carotenoids (peaks at 1156, 1518 cm^{-1}), proteins in β -sheet conformation (peak at 1228 cm^{-1}), lipids and fatty acids including unsaturated fraction (peaks at 1448, 2854 and 3012 cm^{-1}), phosphorylated amino acids and proteins (peak at 1586 cm^{-1}) and proteins (peak at 2935 cm^{-1}).

The negative signals for DNA/RNA, saturated fatty acids, proteins in β -sheet conformation, phosphorylated amino acids and proteins shown in Fig. 2 confirm that for the cancerous tissue overexpression of proteins, high level of nucleic acids associated with cancer development and metastasis, phosphorylation of amino acids and proteins and changes in proteins conformation associated with cancer development are easily observed in vibrational spectra by Raman spectroscopy and imaging.

Additionally, one can see from Fig. 2 that for the noncancerous tissue peaks at ca. 730-772 and 1332 cm^{-1} are observed. These two peaks confirm clearly the α -helix structure of proteins. Simultaneously for this type of sigmoid mucosa one cannot observe any peaks in the spectral range 1235-1240 cm^{-1} , which confirms the lack of β -sheet proteins structure in the noncancerous colon tissue. Summarizing the detailed inspection in Fig. 2 shows that the α -helix structure of proteins is typical for the noncancerous human colon mucosa while peaks characteristic for the β -sheet structure can be observed for the cancerous one. These findings are in agreement with observations whose confirm that β -sheet structure or the lack of the α -form of proteins are typical for various diseases such as prion related diseases, Alzheimer disease related to presence of β -amyloid, β -thalassemia related to the lack of α -hemoglobine stabilizing protein, cancer changes including head and neck or brain cancer [6, 10, 11, 19-21].

Secondly DNA content (peaks at ca. 751, 1342 cm^{-1}) and DNA methylation (red shifts observed for peaks in high frequency region compared to noncancerous tissue 2935, 2964 cm^{-1}) also can be recognized as molecular alterations in human colon cancer. It has been proved that DNA methylation in cancer development plays a variety of roles, including the change of the normal regulation of gene expression. In colorectal cancers about 600 to 800 genes are transcriptionally silenced, compared to normal-appearing tissues, by CpG island methylation [22]. DNA methylation regulates gene expression by recruiting proteins involved in gene repression or by inhibiting the binding of transcription factors to DNA. As a result, the dynamic process involving both *de novo* DNA methylation and demethylation can be observed and consequently cells can develop a stable and unique DNA methylation pattern that regulates tissue-specific gene transcription. Moreover, DNA methylation may be predictor of metastatic or aggressive cancer stage. Therefore, the knowledge of DNA methylation as a driving force in colon cancer development should be an emerging value especially for the clinic practice [23]. The important role of DNA methylation of histones has been proved also for breast cancer by Abramczyk and coworkers [5].

The increase of Raman scattering at 751 cm^{-1} for cancerous mucosa correlates also with a spectacular increase of Raman peak intensity at 1586 cm^{-1} , which describes proteins phosphorylation. It means that huge difference between noncancerous and cancerous tissues on Figure 2 is also seen for signals typical for phosphorylated amino acids and proteins. It has been shown that phosphorylation seems to be the most important mechanism for regulation of protein activity. Abnormal phosphorylation has been observed in many cancers and has driven the development of kinase inhibitors that have utility in a number of cancer subtypes [10, 11, 24-26]. Phosphorylation of proteins involves the enzymatically mediated addition of a

phosphate group (PO_4^{3-}) to its amino acid side chains. Phosphorylated proteins were observed as far back as the early 1900s, but until the 1950s there was not known that phosphorylation is a reversible, enzymatically mediated process, capable of modifying the function of proteins. In general, phosphorylation and dephosphorylation, occur thanks to 2 key enzymes. Protein kinases phosphorylate proteins by transferring a phosphate group from adenosine triphosphate to their target protein. This process is balanced by the action of protein phosphatases, which can subsequently remove the phosphate group. The amount of phosphate that is associated with a protein is therefore precisely determined by the relative activities of the kinase and phosphatase. At the level of a single protein, the binding of a negatively charged phosphate group can lead to changes in the structure of a protein, which alter the way of its functions [24-26]. The phosphorylation of a protein can also target it for degradation and removal from the cell by the ubiquitin-proteasome system. In addition to proteins, other kinds of molecules can also be phosphorylated. In particular, the phosphorylation of lipids, such as phosphatidylinositol-4,5-bisphosphate (PIP2), at various positions on their inositol ring, also plays a key role in signal transduction. Summarizing phosphorylation plays a key role in regulating many intracellular processes that's why, any perturbations in the phosphorylation process can drive many hallmarks of cancer especially cell growth and proliferation.

Lipid phenotype in colon cancer is also very promising as a biomarker of pathological changes. Figure 2 confirms that unsaturated lipids are typical for noncancerous sigmoid mucosa while increasing content of saturated lipid fraction can be treated as a molecular marker of cancerogenesis. Disturbed ratio of unsaturated and saturated lipids seems to be a universal marker of pathogenesis, which can be used for breast, head and neck, brain and colon cancer diagnostics [6,7,10,11].

The huge difference between noncancerous and cancerous sigmoid human mucosa can be seen also for peaks typical for carotenoids (peaks at 1156, 1518 cm^{-1}). The dominant presence of β -carotene in the noncancerous human colon tissue shows that carotenoids as natural antioxidants have anti-cancer benefits and are able to effectively decrease the influence of oxidative stress on colon tissue homeostasis. It has been proved that carotenoids have numerous biological properties and can be considered as chemopreventive agents, the special role of carotenoids in breast cancer diagnostics has been shown by Abramczyk group [7, 27]. For β -carotene in colon cancer it has been published that incorporating of carotenoids foods into the diet may help to reduce the risk of developing cancer [28-30].

To visualize the differences in chemical composition typical for noncancerous and cancerous human sigmoid mucosa we have calculated some ratios typical for proteins, lipids,

carotenoids, sensitivity and specificity of Raman biomarkers, which are presented in Table 2. Table 2 shows also the sensitivity and specificity (for cross validation) obtained using PLSDA analysis for all Raman ratios.

Ratio	Assignment	Noncancerous human sigmoid colon mucosa	Cancerous human sigmoid colon mucosa	Sensitivity	Specificity
751/1156	DNA/Carotenoids	0.14±0.05	1.27±0.07	100%	100%
1228/1332	β-sheet/α-helix proteins conformation	0.88±0.04	1.11±0.07	100%	100%
1586/1004	Phosphorylated proteins/proteins	0.73±0.14	2.57±0.09	100%	100%
2854/2935	Lipids/proteins	0.96±0.06	0.24±0.02	100%	100%

Table 2 The Raman intensity ratios: I_{751}/I_{1156} ; I_{1228}/I_{1332} ; I_{1586}/I_{1004} ; I_{2854}/I_{2935} for all analyzed sigmoid mucosa samples, sensitivity and specificity for Raman biomarkers

Figure 3 shows the schematic representation of the Raman intensity ratios: I_{751}/I_{1156} ; I_{1228}/I_{1332} ; I_{1586}/I_{1004} ; I_{2854}/I_{2935} for all analyzed sigmoid mucosa samples

Fig. 3. The schematic representation of the Raman intensity ratios: I_{751}/I_{1156} ; I_{1228}/I_{1332} ; I_{1586}/I_{1004} ; I_{2854}/I_{2935} for all analyzed sigmoid mucosa samples.

One can see from Table 2 and Fig. 3 that cancerous tissue of sigmoid mucosa contains incomparably more DNA, β-sheet proteins, phosphorylated proteins, which prove that cell metabolism and conformational structure of the most important chemical components of sigmoid mucosa are for noncancerous and cancerous tissues significantly different.

For a cancerous human colon sample, we have performed not only analysis of *en face* tissue specimen, but we have performed also analysis for cross-section. Analysis of such a sample allows us to investigate some layers illustrated in Sch.1. Figure 4 presents Cluster Analysis of cancerous sigmoid human colon sample.

Fig.4 Microscopy image (A), Raman image (200x800 μm, spatial resolution 2 μm, integration time 0.3 sec.) based on Cluster Analysis (B) and average Raman spectra typical for all clusters seen on (B) for the cross section of the cancerous sigmoid human mucosa, patient PB.

One can see from Fig. 4 that once again Raman imaging of the cancerous tissue is dominated by areas typical for proteins (2935 cm^{-1}), phosphorylated proteins (1586 cm^{-1}), saturated lipids (1127 cm^{-1}), β -sheet form proteins (1231 cm^{-1}).

The analysis of the cross-section allows us also to track changes in concentration of different chemical compounds of the sigmoid tissue layers illustrated in Sch.1.

Figure 5 presents the scheme of Raman spectra analysis and the radial distribution functions of concentration of different components of the cancerous sigmoid tissue sample as a function of the distance from the center of the sigmoid lumen.

One can see that going from the empty lumen to its outer wall we can observe several areas separated by the maxima. The first maximum is observed at around $5\text{ }\mu\text{m}$ and the second one at around $250\text{ }\mu\text{m}$. These maxima correspond well with borders of orange and red areas seen in Fig. 4.

Fig. 5. Microscopy image of cancerous human sigmoid tissue, red line indicates the direction along which the Raman spectra were recorded (A) radial distribution function for lipids, proteins and phosphorylated proteins based on Raman bands typical for selected tissue components (B).

Recently we have proved that such an analysis is very effective in the analysis of human milk duct showing an asymmetric concentration of different chemical components for normal tissue and reverse gradients dependence for cancerous one [4].

We have demonstrated that Raman imaging and spectroscopy are capable of identification of sigmoid cancer based on Raman spectra typical for noncancerous and cancerous human mucosa. This is particularly valuable in the context of endoscopic screening based on Raman biomarkers. Our studies have proved that some specific alterations in lipids/proteins/phosphorylated proteins/carotenoids contents show the potential to provide predictive cancer markers indicating simultaneous directions of targeted treatment.

4. Conclusion

Raman spectroscopy and imaging are powerful techniques to distinguish between noncancerous and cancerous human sigmoid colon mucosa. DNA, lipids, proteins and carotenoids can be treated as biomarkers of cancerogenesis. Ratios: $751/1156$ (DNA/Carotenoids), $1228/1332$ (β -sheet/ α -helix proteins conformation), $1586/1004$ (Phosphorylated proteins/Proteins), $2854/2935$ (Lipids/Proteins) can be used to differentiate noncancerous and cancerous human sigmoid colon mucosa based on Raman spectroscopy and

imaging. Measurement of a single Raman spectrum allows the diagnosis of cancer changes based on several biomarkers simultaneously (ratios described above) without removing any tissues from the patient's body. Analysis of tissue cross-section through sigmoid layers based on Raman spectra can be used to estimate the concentration of different chemical components of human colon tissues without any external staining.

Despite numerous advantages, there are also many challenges in clinical applications of the Raman spectroscopy based techniques. First of all, there is a need of the standardization of protocols for sample preparation. The spectroscopic analysis protocols must be primarily guided first and foremost by the demands of current clinical practice. Validation of the robustness Raman spectroscopy protocols through inter laboratory cross checking of the results is also crucial for the practical applications. The sharing of the increasingly complex data sets is the other rapidly emerging requirement. The data preprocessing is undoubtedly the next "hot issue" of ongoing debates in interdisciplinary scientists and clinicians groups. The other question regards the quality of the instrumentation and a minimum modes required for the clinical Raman based systems, which is complicated since it very much depends on the type of the analyzed specimen (different for in-vivo measurements (in operating room) and ex-vivo (in pathology laboratory)).

Abbreviations

CA: Cluster Analysis; HE: Haematoxylin and Eosin stain

Funding

The project was funded through The National Science Centre Poland Grant UMO-2017/25/B/ST4/01788.

Ethics approval and consent to participate

All tissue procedures were conducted under a protocol approved by the institutional Bioethical Committee at the Medical University of Lodz, Poland (RNN/323/17/KE/17/10/2017). Written informed consent was obtained from patients.

Competing interests

The authors declare that they have no competing interests.

References

- [1] F.M. Lyng, D. Traynor, I.R.M. Ramos, F. Bonnier, H.J. Byrne, Raman spectroscopy for screening and diagnosis of cervical cancer, *Bioanal. Chem.* 27 (2015) 1-11.
- [2] Z. Huang, A. McWilliams, H. Lui, D.I. McLean, S. Lam, H. Zeng, Near-infrared Raman spectroscopy for optical diagnosis of lung cancer, *Int J Cancer.* 6 (2003) 1047–1052.
- [3] G.V. Nogueira, L.S. Silveira, A.A. Martin, R.A. Zângaro, M.T. Pacheco, M.C. Chavantes, C.A. Pasqualucci, Raman spectroscopy study of atherosclerosis in human carotid artery. *J. Biomed. Opt.* 3 (2005) 1-7.
- [4] H. Abramczyk, B. Brozek-Pluska, M. Kopec, Polarized Raman microscopy imaging: capabilities and challenges for cancer research, *J Mol Liq.* 245 (2017) 52-61.
- [5] B. Brozek-Pluska, M. Kopec, H. Abramczyk, Development of a new diagnostic Raman method for monitoring epigenetic modifications in the cancer cells of human breast tissue, *Anal. Methods.* 8 (2016) 8542-8553.
- [6] B. Brozek-Pluska, M. Kopec, Raman microspectroscopy of Hematoporphyrins. Imaging of the noncancerous and the cancerous human breast tissues with photosensitizers, *Spectrochim. Acta A.* 169 (2016) 182–191.
- [7] H. Abramczyk, B. Brozek-Pluska, New look inside human breast ducts with Raman imaging. Raman candidates as diagnostic markers for breast cancer prognosis: Mammaglobin, palmitic acid and sphingomyelin, *Anal. Chim. Acta.* 909 (2016) 91-100.
- [8] S. Li, L. Li, Q. Zeng, Y. Zhang, Z. Guo, Z. Liu, M. Jin, C. Su, L. Lin, J. Xu, S. Liu, Characterization and noninvasive diagnosis of bladder cancer with serum surface enhanced Raman spectroscopy and genetic algorithms, *Sci. Rep.* 5 (2005) 1-7.
- [9] N. Sharma, N. Takeshita, K.Y. Ho, Raman spectroscopy for the endoscopic diagnosis of esophageal, gastric, and colonic diseases, *Clin Endosc.* 5 (2016) 404-407.
- [10] H. Abramczyk, A. Imiela, The biochemical, nanomechanical and chemometric signatures of brain cancer, *Spectrochim. Acta A.* 188 (2018) 8-19.
- [11] H. Abramczyk, A. Imiela, A. Śliwińska, Novel strategies of Raman imaging for exploring cancer lipid reprogramming, *J. Mol. Liq.* 274 (2019) 52-59.
- [12] M. Jermyn, J. Mercier, K. Aubertin, J. Desroches, K. Urmey, J. Karamchandiani, E. Marple, M.C. Guiot, F. Leblond, K. Petrecca, Highly accurate detection of cancer in situ with intraoperative, label-free, multimodal optical spectroscopy, *Cancer Res.* 14 (2017) 3942-3950.

- [13] S. Dochow, D. Ma, I. Latka, T. Bocklitz, B. Hartl, J. Bec, H. Fatakdawala, E. Marple, K. Urmeý, S. Wachsmann-Hogiu, M. Schmitt, L. Marcu, J. Popp, Combined fiber probe for fluorescence lifetime and Raman spectroscopy, *Anal. Bioanal. Chem.* 27 (2015) 8291-8301.
- [14] *Onkologia. Podręcznik dla studentów i lekarzy* ed. R. Kordek, VIA Medica, Gdansk, 2013.
- [15] M.G. Shim, L.M. Wong Kee Song, N.E. Marcon, B.C. Wilson, In vivo near-infrared Raman spectroscopy: demonstration of feasibility during clinical gastrointestinal endoscopy, *Photochem. Photobiol.* 1 (2000) 146–150.
- [16] P.O. Andrade, R.A. Bitar, K. Yassoyama, H. Martinho, A.M.E. Santo, P.M. Bruno, A.A. Martin, Study of normal colorectal tissue by FT-Raman spectroscopy, *Anal. Bioanal. Chem.* 5 (2007) 1643–1648.
- [17] C. Krafft, A.A. Ramoji, C. Bielecki, N. Vogler, T. Meyer, D. Akimov, P. Rösch, M. Schmitt, B. Dietzek, I. Petersen, A. Stallmach, J. Popp, A comparative Raman and CARS imaging study of colon tissue, *J. Biophoton.* 5 (2009) 303–312.
- [18] L. Mavarani, D. Petersen, S.F. El-Mashtoly, A. Mosig, A. Tannapfel, C. Kötting, K. Gerwert, Spectral histopathology of colon cancer tissue sections by Raman imaging with 532 nm excitation provides label free annotation of lymphocytes, erythrocytes and proliferating nuclei of cancer cells, *Analyst.* 14 (2013) 4035-4039.
- [19] R.K. Murray, D.K. Granner, V.W. Rodwell *Harpers Illustrated Biochemistry*, The Mc Graw-Hill Companies, Inc. New York, 2006.
- [20] S.B. Prusiner, Molecular biology of prion diseases, *Science.* 5012 (1991) 1515-1522.
- [21] M.R. Goldsworthy, A.M. Vallence, The role of β -amyloid in Alzheimer's disease-related neurodegeneration, *J. Neurosci.* 32 (2013) 12910-12911.
- [22] Y.P. Wang, Q.Y. Lei, Metabolic recoding of epigenetics in cancer, *Cancer Commun (Lond).* 1 (2018) 25.
- [23] M.S. Kim, J. Lee, D. Sidransky, DNA methylation markers in colorectal cancer, *Cancer Metastasis Rev.* 1 (2010) 181-206.
- [24] E.A. Vucic, K.L. Thu, K. Robison, L.A. Rybaczyk, R. Chari, C.E. Alvarez, W.L. Lam, Translating cancer “omics” to improved outcomes, *Genome Res.* 2 (2012) 188-195.
- [25] P. Radivojac, P.H. Baenziger, M.G. Kann, M.E. Mort, M.W. Hahn, S.D. Mooney, Gain and loss of phosphorylation sites in human cancer. *Bioinformatics.* 16 (2008) 241-247.

- [26] C. Greenman, R. Wooster, P.A. Futreal, M.R. Stratton, D.F. Easton, Statistical analysis of pathogenicity of somatic mutations in cancer, *Genetics*. 4 (2006) 2187-2198.
- [27] B. Brozek-Pluska, M. Kopec, J. Surmacki, H. Abramczyk, Raman microspectroscopy of noncancerous and cancerous human breast tissues. Identification and phase transitions of linoleic and oleic acids by Raman low-temperature studies, *Analyst*. 7 (2015) 2134-2143.
- [28] M.L. Slattery, J. Benson, K. Curtin, K.N. Ma, D. Schaeffer, J.D. Potter, Carotenoids and colon cancer, *Am. J. Clin. Nutr.* 2 (2000) 575–582.
- [29] K.A. Steinmetz, J.D. Potter, Vegetables, fruit, and cancer. I. Epidemiology, *Cancer Causes Control*. 5 (1991) 325–357.
- [30] J.D. Potter, M.L. Slattery, R.M. Bostick, S.M. Gapstur, Colon cancer: a review of the epidemiology. *Epidemiol Rev.* 2 (1993) 499–545.

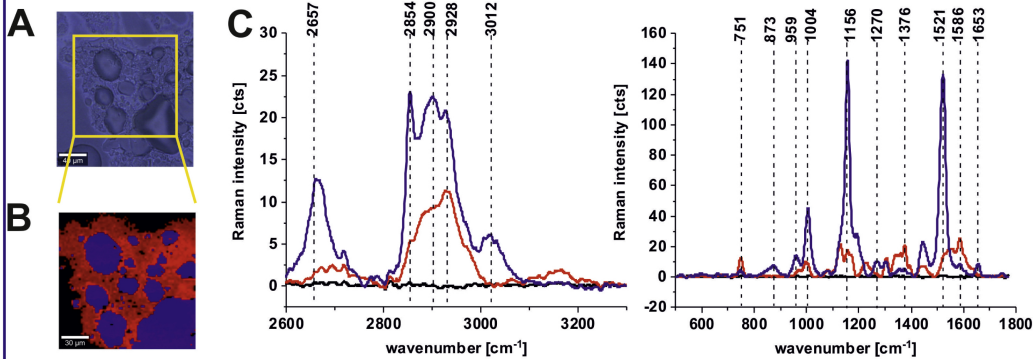
Author Statement

Abramczyk H.: Conceptualization, Methodology, Data analysis, Reviewing, Supervision; **Brozek-Pluska B.:** Data measurements, Data analysis, Original draft preparation, Reviewing and Editing. **Dziki A.:** Reviewing, Supervision.

Highlights:

- Colon cancer changes can be detected by Raman spectroscopy and imaging.
- DNA, lipids, proteins and carotenoids are treated as biomarkers of carcinogenesis.
- Different biomarkers can be simultaneously analyzed by Raman spectroscopy.
- Human colon tissues can be characterized without external staining.

I. noncancerous tissue



II. cancerous tissue

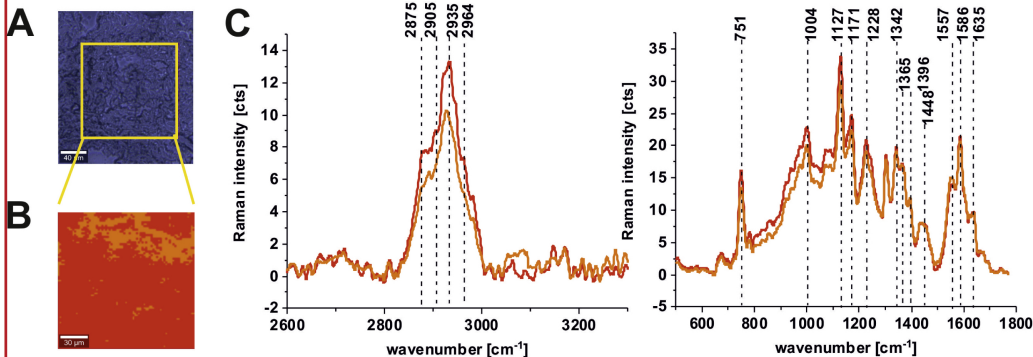


Figure 1

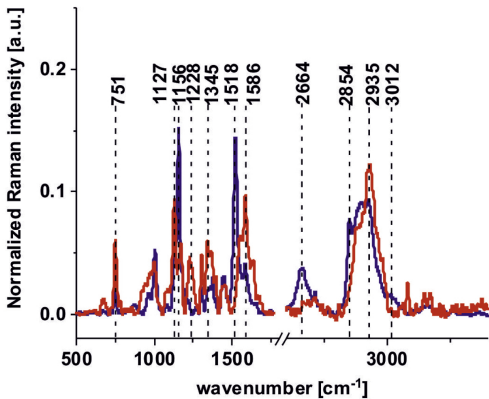
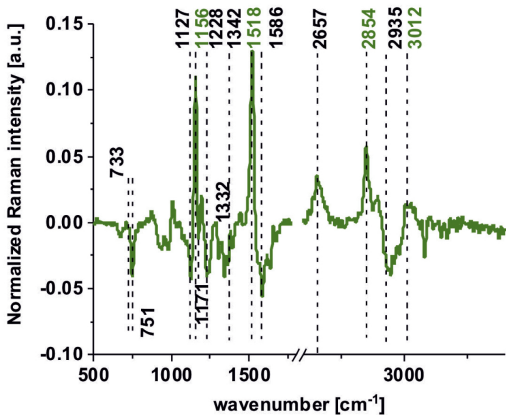
A**B**

Figure 2

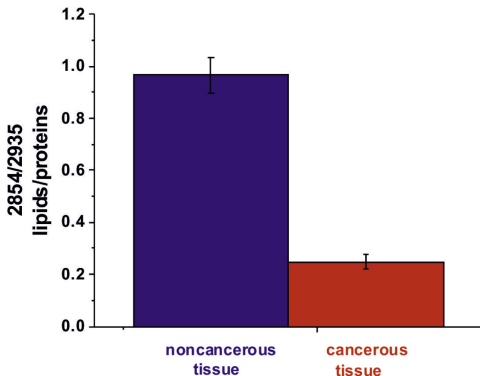
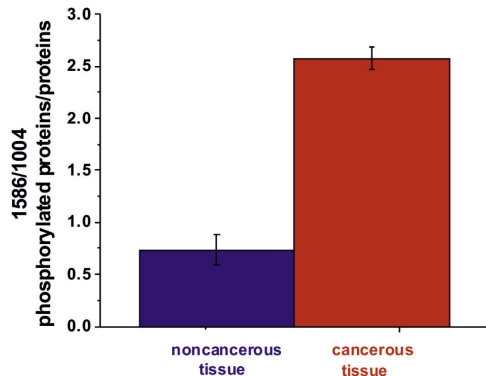
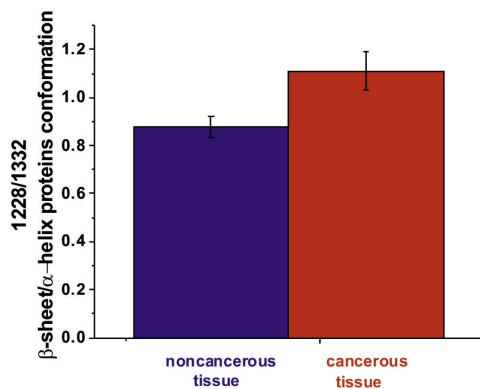
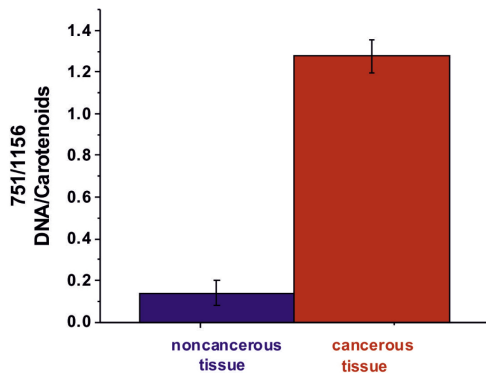


Figure 3

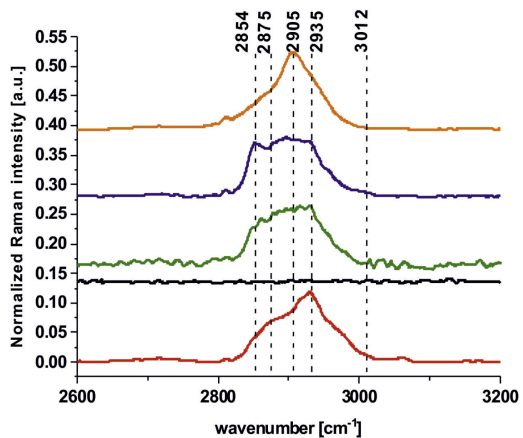
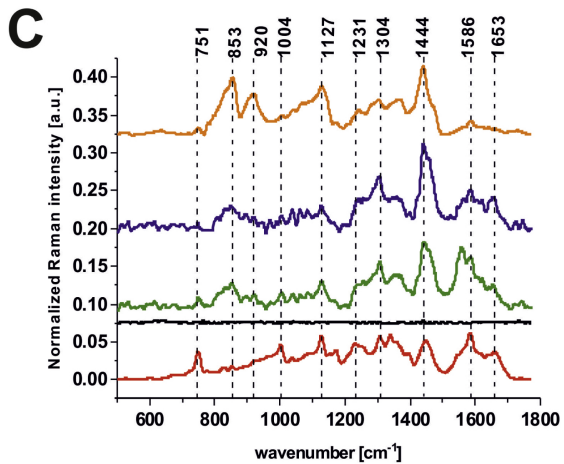
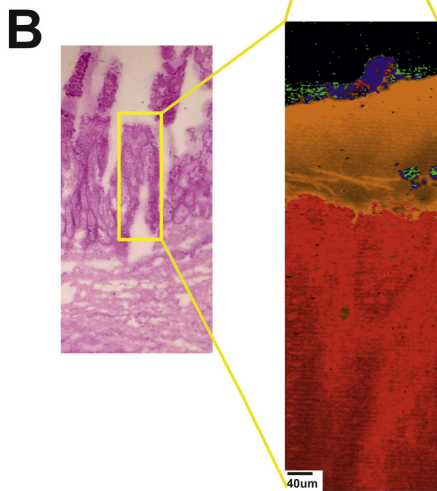


Figure 4

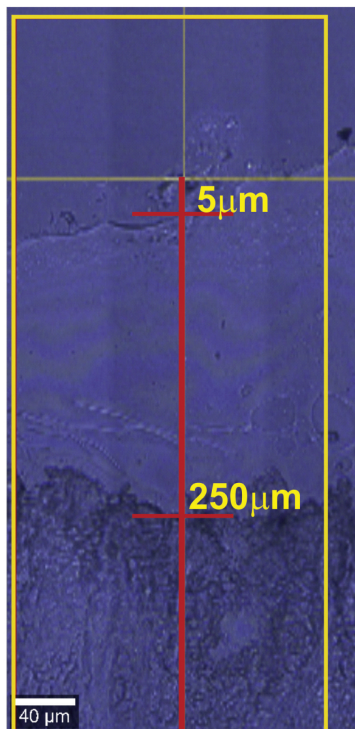
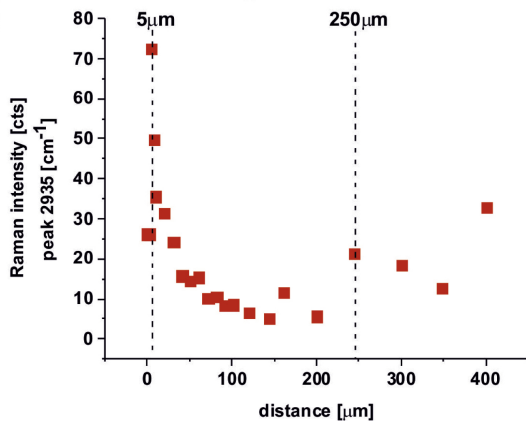
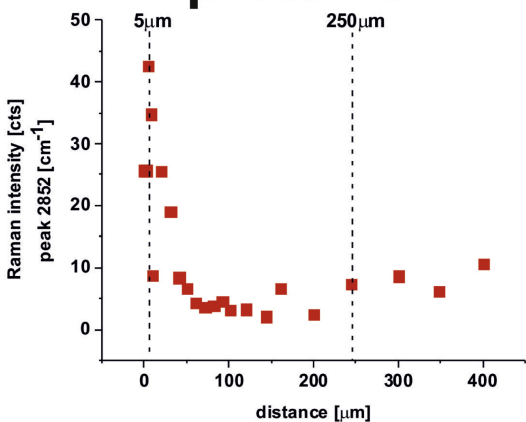
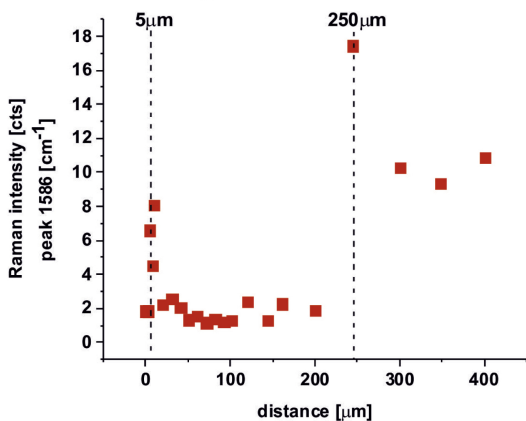
A**B****lipids****proteins****phosphorylated proteins**

Figure 5